American Journal of Pathology, Vol. 165, No. 1, July 2004

Prion Protein Accumulation and Neuroprotection in Hypoxic Brain Damage

Neil F. McLennan,* Paul M. Brennan,† Alisdair McNeill,† Ioan Davies,‡ Andrew Fotheringham,‡ Kathleen A. Rennison,* Diane Ritchie,§ Francis Brannan,† Mark W. Head,* James W. Ironside,* Alun Williams,§ and Jeanne E. Bell†

From the National Creutzfeldt-Jakob Disease Surveillance Unit and Pathology (Neuropathology),† School of Molecular and Clinical Medicine, University of Edinburgh, Edinburgh; the Biological Gerontology Group,‡ School of Medicine and School of Biological Sciences, University of Manchester, Manchester; and the Neuropathogenesis Unit,§ Institute for Animal Health, Edinburgh, United Kingdom*

The function of the normal conformational isoform of prion protein, PrP^C, remains unclear although lines of research have suggested a role in the cellular response to oxidative stress. Here we investigate the expression of PrP^C in hypoxic brain tissues to examine whether PrP^C is in part regulated by neuronal stress. Cases of adult cerebral ischemia and perinatal hypoxic-ischemic injury in humans were compared with control tissues. PrP^C immunoreactivity accumulates within neuronal processes in the penumbra of hypoxic damage in adult brain, and within neuronal soma in cases of perinatal hypoxic-ischemic injury, and *in situ* hybridization analysis suggests an upregulation of PrP mRNA during hypoxia. Rodents also showed an accumulation of PrP^C in neuronal soma within the penumbra of ischemic lesions. Furthermore, the infarct size in PrP-null mice was significantly greater than in the wild type, supporting the proposed role for PrP^C in the neuroprotective adaptive cellular response to hypoxic injury. *(Am J Pathol 2004, 165:227–235)*

An abnormal isoform of the prion protein, PrP^{Sc}, is thought to be the major or even the sole component of the prion, the novel infectious agent implicated in transmission and pathogenesis of transmissible spongiform encephalopathies, or prion diseases.[1] The prion protein isoform found in normal tissues, PrP^C, is a copper-binding sialoglycoprotein tethered to the cell surface by way of a glycosylphosphatidylinositol anchor that is expressed predominantly in neurons,[2–4] and to a lesser degree in some extra neuronal tissues, such as cardiac muscle, lymphoid tissues, skin, and gastrointestinal myenteric ganglion cells.[5–8]

Studies of mice ablated for the prion protein gene ($PrP^{0/0}$), have shown it to be nonessential for viability.[9] PrP^C has been implicated in cell-cell signaling, cell adhesion, and other cell-specific roles, for example, during embryogenesis.[10–12] Others have suggested that it may have a specific neuronal role, supported by its presynaptic location in axonal terminals,[13] for example, in regulation of circadian rhythm[14,15] or $GABA_A$-receptor-mediated fast inhibition.[16] More recently PrP^C has been proposed to have a role in the cellular defense against oxidative stress. Pheochromocytoma cells selected for resistance to oxidative stress express higher levels of PrP^C than wild-type cells.[17] Moreover, tumor prostate spheroids subjected to increasing oxidative stress display increased PrP^C expression,[18] as do NT-2 cells exposed to heat shock,[19] and cerebellar cells from $PrP^{0/0}$ mice are more susceptible to oxidative stress than are wild-type cells,[20,21] and studies with $PrP^{0/0}$ mice have shown increased levels of oxidative stress markers *in vivo* compared to wild-type animals.[22–24] Additionally, it has been suggested that the pathogenesis of prion diseases could in part be because of a loss of PrP^C function in the management of oxidative stress.[25–27]

When hypoxic damage occurs, oxidative stress is a potentially important cause of cellular injury and death. In mounting protective responses, cells may differentially express a number of proteins, including antioxidants, which limit the damage and initiate repair processes.[28,29] If PrP^C does have an antioxidant role, it might be induced in response to oxidative stress in neurons. To examine our hypothesis we chose cerebral ischemia (CI) and perinatal hypoxic-ischemic injury (HII) as common human disorders exhibiting oxidative stress responses in the central nervous system, as well as a mouse model of CI, and used immunohistochemical and *in situ* hybridization analyses to compare PrP^C expression in hypoxic and nonhypoxic brain tissue sections.

Supported by the Medical Research Council (G9627376), the European Union (EC Biotech 4-98-6064), the University of Edinburgh (Faculty of Medicine Vacation grant to P.B.), and the Welcome Trust (Vacation Research scholarship to A.M.).

Accepted for publication March 30, 2004.

Current address of A.W.: Royal Veterinary College, London, UK.

Address reprint requests to Neil F. McLennan, School of Molecular and Clinical Medicine, Molecular Medicine Centre (CRUK Labs), University of Edinburgh, Western General Hospital, Crewe Rd., Edinburgh, EH4 2XU UK. E-mail: n.mclennan@ed.ac.uk.

Table 1. Adult Cerebral Ischemia Case Details

Case no.	Age	Sex	Relevant diagnosis	PM interval (hours)	Affected hemisphere	Time of symptoms to death
A1	87	F	Multiple recent cerebral infarcts	72	Bilateral	14 days
A2	79	F	Multiple cerebral infarcts	24	Bilateral	<24 hours
A3	57	F	Recent cerebral infarction	96	Left	7 days
A4	87	M	Old cerebral watershed infarction	48	Left	40 days
A5	42	F	Recent cerebral infarction	24	Left	6 days
A6	50	F	Extensive recent cerebral infarction	48	Bilateral	10 days
A7	84	F	Acute cerebral infarction (1 to 2 days old)	24	Left	<36 hours
A8	85	F	Recent infarct superimposed upon old infarct	72	Right	40 days
A9	69	M	Recent cerebral infarction	24	Right	28 days
A10	84	M	Acute cerebral infarction	48	Left	<24 hours
A11	68	F	Recent multiple cerebral infarcts	24	Bilateral	37 days
A12	90	M	Recent cerebral infarction	48	Right	12 days

Materials and Methods

Cases for Study

Autopsy records were used to identify cases in which clinical history and postmortem neuropathological examination indicated that recent cerebral infarction had occurred and directly contributed toward death. Formalin-fixed, paraffin-embedded tissues from 12 such cases were obtained from the Department of Pathology (Neuropathology), School of Clinical and Molecular Medicine, University of Edinburgh, Edinburgh. Samples from these cases were processed at postmortem with a fixation regime of at least 2 weeks in 10% neutral formalin followed by paraffin embedding. The range of ages of the cases was 42 to 90 years, postmortem intervals were 24 to 72 hours, and the delay between onset of symptoms to death was <24 hours to 40 days. Details of the cases are summarized in Table 1. The brain regions studied varied between cases depending on the site of infarction and included both white and gray matter regions. Three tissue blocks containing infarcts were available for case number A1 whereas single blocks represented the rest of the cases. The perinatal HII series consisted of five cases in which cerebral hypoxia was diagnosed on postmortem microscopic examination, and brain tissues from three perinatal cases that did not display neuropathological injury were used as negative controls. Hypoxic cases are summarized in Table 2.

The presence of prion disease in all cases was excluded on the basis of clinical history and subsequent histological examination. From our extensive research experience it is known that no accumulations of PrP^C immunoreactivity are found in neurologically normal brain tissues, and so tissue blocks from normal brain regions in each case were used as negative controls for PrP^C detection and a case of Alzheimer's disease, previously shown to be positive within plaques for PrP^C and β amyloid precursor protein (βAPP) immunoreactivity, was used as a positive control. All tissue samples used in this research were coded and anonymized. This study was approved by the Lothian Research Ethics Committee.

CI in Mice

All mice used in this study were a kind gift from J. Manson (Institute for Animal Health, Edinburgh, UK). The role of PrP in ischemic brain damage was investigated in adult male wild-type 129/Ola ($PrP^{+/+}$) mice, inbred PrP-null mice 129/Ola ($PrP^{0/0}$), and the heterozygous cross. Focal CI was induced by electrocoagulation of the left middle cerebral artery (MCA)[30] and mice were studied 24 hours later. This procedure, with the electrocautery consistently performed at the same site, produces a highly reproducible pattern of brain damage with little, or no, mortality. Body temperature was maintained at 37°C throughout surgery and the postoperative recovery. Twenty-four

Table 2. Perinatal Hypoxia Case Details

Case no.	Age	Sex	Relevant diagnosis	PM interval (hours)
P1	6 months	M	Acute cerebral hypoxia	<24
P2	14 days	M	Recent global hypoxia	<24
P3	9 weeks	M	Cortical infarction and neuronal hypoxia	<24
P4	Still born; 38-weeks gestation	M	Ongoing global hypoxia	<24
P5	2 days	F	Widespread cortical infarction and hypoxic damage	72

Table 3. Primary Antibodies, Dilutions, Incubation Conditions, and Antigen Retrieval Methods

Antibody	Antigen	Source	Antigen retrieval	Dilution factor	Incubation conditions
3F4	PrP; aa 108 to 111	DAKO	HA/FA	1:50	4°C o/n or RT 60 min
R9	PrP; aa 89 to 103	R. Kascsak	FA	1:400	RT 60 min
R27	PrP; aa 89 to 103	R. Kascsak	FA	1:400	RT 60 min
MAB348	Pre-A4 βAPP, aa 66 to 81	Chemicon	FA	1:250	RT 90 mins

aa, amino acid range of antigen; HA, hydrolytic autoclaving (121°C for 10 minutes in distilled water); FA, 96% formic acid; o/n, overnight; RT, room temperature.

hours later, the mice were reanesthetized and *trans*-cardiac perfusion performed using either periodate-lysine-paraformaldehyde (final concentration of 2% formaldehyde, pH 7.4, for immunohistochemistry) or with 4% phosphate-buffered formaldehyde (for *in situ* hybridization). In addition, the brains of further mice were either immersion-fixed in formol-saline for *in situ* hybridization studies or were removed fresh for the determination of the infarct size.

Immunohistochemistry

For immunohistochemistry analysis 5-μm sections were cut from fixed brain tissue blocks. Sections were mounted on glass slides (Superfrost Plus; BDH, Poole, UK), dewaxed, rehydrated, and endogenous peroxidases quenched by treatment with 0.3% hydrogen peroxide in methanol for 30 minutes. The primary antibodies, dilutions, incubation conditions, and antigen retrieval methods used in this study are listed in Table 3. Sections from human adult and pediatric brain were treated with both the anti-βAPP antibody MAB348 (Chemicon Int., Temecula, CA) and the anti-PrP monoclonal antibody 3F4 (DAKO, Glostrup, Denmark), diluted in 20% rabbit serum in Tris-buffered saline (20 mmol/L Tris-HCl (pH 7.6), 137 mmol/L NaCl). After primary antibody incubation and washing in Tris-buffered saline, sections were incubated with a biotinylated rabbit anti-mouse antibody (Scottish Antibody Production Unit, Edinburgh, UK) diluted 1:200 in 20% rabbit serum in Tris-buffered saline for 30 minutes. The staining pattern was visualized using the tyramide signal amplification methodology (CSA, DAKO). Sections were counterstained with hematoxylin before mounting in DPX (BDH).

For the murine brain samples, PrP immunohistochemistry was performed on periodate-lysine-paraformaldehyde-fixed, wax-embedded brains using a standard peroxidase-anti-peroxidase method with diaminobenzidine as the chromogen. Sections were pretreated with 98% formic acid for 5 minutes and incubated with rabbit anti-PrP antibodies (antibodies R9 and R27). Rabbit sera and antibodies raised against irrelevant antigens (including rabbit antisera against bacterial antigens) were used as controls for the first antibody. The hemisphere contralateral to the MCA occlusion, and equivalent brain areas of both sham-operated and nonoperated mice, acted as tissue controls. In all cases controls were performed in which the primary antibodies were omitted. Interpretation of the semiquantitative measurements of the immunohistochemistry signals were agreed on by the consensus of several operators. All stained sections were examined microscopically and the images generated using an Olympus DP70 camera and Olympus DP-Soft software.

In Situ *Hybridization*

Tissue sections from both the human perinatal HII case (P3) and murine CI models ($n = 3$) were subjected to *in situ* hybridization analysis using the method described previously.[3] In summary tissue sections were rehydrated, partially digested with proteinase K, and hybridized with human or mouse-specific PrP cRNA probes labeled with digoxigenin (Roche Diagnostics, Lewes, UK). Unduplexed RNA molecules were removed using RnaseA in high salt, followed by washing with increasing stringency. Hybridized sections were treated with anti-digoxigenin Fab fragments labeled with alkaline phosphatase (Roche Diagnostics) and visualized by using nitro blue tetrazolium/5-bromo-4-chloro-3-indolyl phosphate as the chromagen. cRNA molecules complimentary to the test probes served as controls. The developed tissue sections were analyzed and images captured as above. Other sections were stained with 0.1% toluidine blue or 0.1% cresyl violet to show the morphological appearance of the ischemic lesion.

Ischemic Lesion Size Measurement

The ischemic lesion size was assessed in a total of 19 129/Ola (PrP$^{+/+}$) mice, 17 129/Ola (PrP$^{0/0}$) mice, and 6 heterozygous crosses of these, in more than four experiments throughout a 2-year period. The animals were anesthetized with halothane, killed by decapitation, and their brains removed. All brains were coded before sections were cut to ensure that measurements were made blind. Coronal sections, 500 μm thick, were cut using a 735M tissue Vibroslice, and the slices immediately immersed in 0.1% tetrazolium blue chloride (containing 1.25% dimethyl sulfoxide and 2 mmol/L $MgCl_2$ in 0.1 mol/L phosphate buffer, pH 7.4). Slices were incubated for 30 minutes at 37°C after which the infarct was visible as an unstained region of the section. The sections were then fixed in 4% phosphate-buffered formaldehyde (pH 7.4), for a minimum of 24 hours at 0 to 4°C before image analysis. An indirect method was used to calculate infarct volume using a semiautomated image analysis system (Imagan 2; Leitz/Kompira, UK). Three measurements were recorded: 1) *a*, area of the infarct, mm^2; 2) *b*, area of infarcted left hemisphere, mm^2; 3) *c*, area of the non-

ischemic right hemisphere, mm^2. We observed enlargement of the brain hemisphere on the side that had undergone MCA occlusion. To compensate for this increase in the size of the hemisphere the proportional increase in the size of the infarcted lobe was calculated as follows: Proportional increase because of swelling of the hemisphere (d) = ($b - c$)/($b + c$); infarct area (mm^2) corrected for swelling (e) = a/(1 + d); giving the total infarct volume = Σ (e).t (where t is section thickness). The data on infarct size were then calculated as the mean values and SD for each of the three PrP genotypes. An analysis of variance was used to compare the data from successive experiments and significant differences between the groups identified using the Scheffé multiple comparison test.

Vascular Structure Determination—Perfusion with Latex and Indian Ink

Mice were prepared for surgery as described above. The heart was exposed and the animal perfused with heparinized saline until the draining fluids were cleared of red blood cells (usually 1 to 2 ml of saline). The animal was then perfused with a latex solution (Neoprene latex 671A; Omya, UK) containing 10% waterproof Indian ink. The animal was decapitated and the brain carefully dissected from the skull using fine dissecting scissors and fixed by immersion in 4% phosphate-buffered paraformaldehyde for visual analysis. Four mice of each genotype were used for the analysis

Results

Adult CI Cases

The adult CI cases examined in this series displayed areas of focal infarction involving both gray and white matter, with typical vascular lesions circumscribed by PrP immunoreactivity within swollen axonal bulbs together with a punctate background staining pattern (Figure 1). This PrP-penumbral-staining phenomenon was demonstrated within serial sections of the same hypoxic foci. Overall 10 of the 12 cases showed infarct-associated PrP immunoreactivity although the staining intensity varied between cases and heterogeneous patterns of PrP deposition were seen (cases A2 and A9 were PrP-negative). Of these 10 cases all showed a high degree of punctate PrP staining (Figure 1, f to i, with h as a control), whereas 5 of the cases showed large amounts of axonal staining (cases A1, A3, A4, A7, and A12) (Figure 1e), although positive axons were seen in all cases.

In serial sections taken from areas of adult hypoxic white matter brain damage, βAPP immunoreactivity was seen in axons within the penumbra of hypoxic damage with a similar pattern of distribution to the prion protein axonal positivity. Areas of necrotic white matter at the center of these infarcts appeared negative for both PrP and βAPP (Figure 1; b to d). Serial sections demonstrated that βAPP immunoreactivity was invariably present in axons immunoreactive for prion protein. In cases with gray matter lesions, similar patterns of PrP deposition were seen (Figure 1j), and in addition PrP-positive neuronal soma (morphologically identified) were detected. Here immunopositivity was found to exist in spatially distinct clusters and undamaged adjacent brain areas did not show such PrP-expressing cells (Figure 1k). Control tissues and nondamaged regions from the test cases did not show any such positive staining for PrP or βAPP.

The length of the postmortem interval did not seem to correlate with the degree of PrP staining with both short (24 hours) and long (72 hours) intervals resulting in varying degrees of staining. The same was true for the disease duration with both long and short durations resulting in variable degrees of staining. The two cases that showed no infarct-associated PrP staining (A2 and A9) differed in disease duration (A2 $<$ 24 hours, A9 = 28 days). Other cases with similar disease time frames (cases A7 and A10, short duration; A4, A8, and A11, longer duration) were strongly positive for PrP.

Perinatal HII Cases

In the perinatal cases, hypoxic regions were identified by the presence of eosinophilic neurons and reactive microglia. All cases studied showed PrP staining associated specifically with the hypoxic regions. The majority of immunostained cells occurred in clusters and were morphologically identified as neurons (Figure 2, a and b). Prion protein immunostaining was not demonstrated in nonhypoxic control tissue, nor was it present in undamaged regions within the hypoxic cases. The pediatric cases differed from the adult ones in that the PrP staining was primarily within the neuronal soma rather than axonal.

To address the question of PrP expression in hypoxic tissue *in situ* hybridization analysis was performed. Because of the strictly limited amounts of tissue available a single case of perinatal HII (case P3) was used. A marked increase in PrP mRNA levels in the neuronal soma within brain regions that also demonstrated PrP^C accumulation was seen relative to the surrounding tissue where only moderate PrP expression was visible at the given exposure (Figure 2, c and d). No cell types other than neurons were found to be expressing PrP mRNA at detectable levels.

Murine Stroke Model

In this study, permanent MCA occlusion caused reproducible damage in each strain of mouse but no major neurological deficits, or mortality, were observed throughout the 24-hour period after the onset of ischemia. The size, severity, and pattern of lesion was consistent within each PrP genotype of mouse of mice studied (Table 4).

The Appearance and Size of the Infarct in PrP Wild-Type, Null, and Heterozygous Mice

Examination of toluidine blue-stained sections showed ischemic brain damage in the $PrP^{+/+}$, $PrP^{+/0}$, and the $PrP^{0/0}$ mice (serial coronal sections shown in Figure 3).

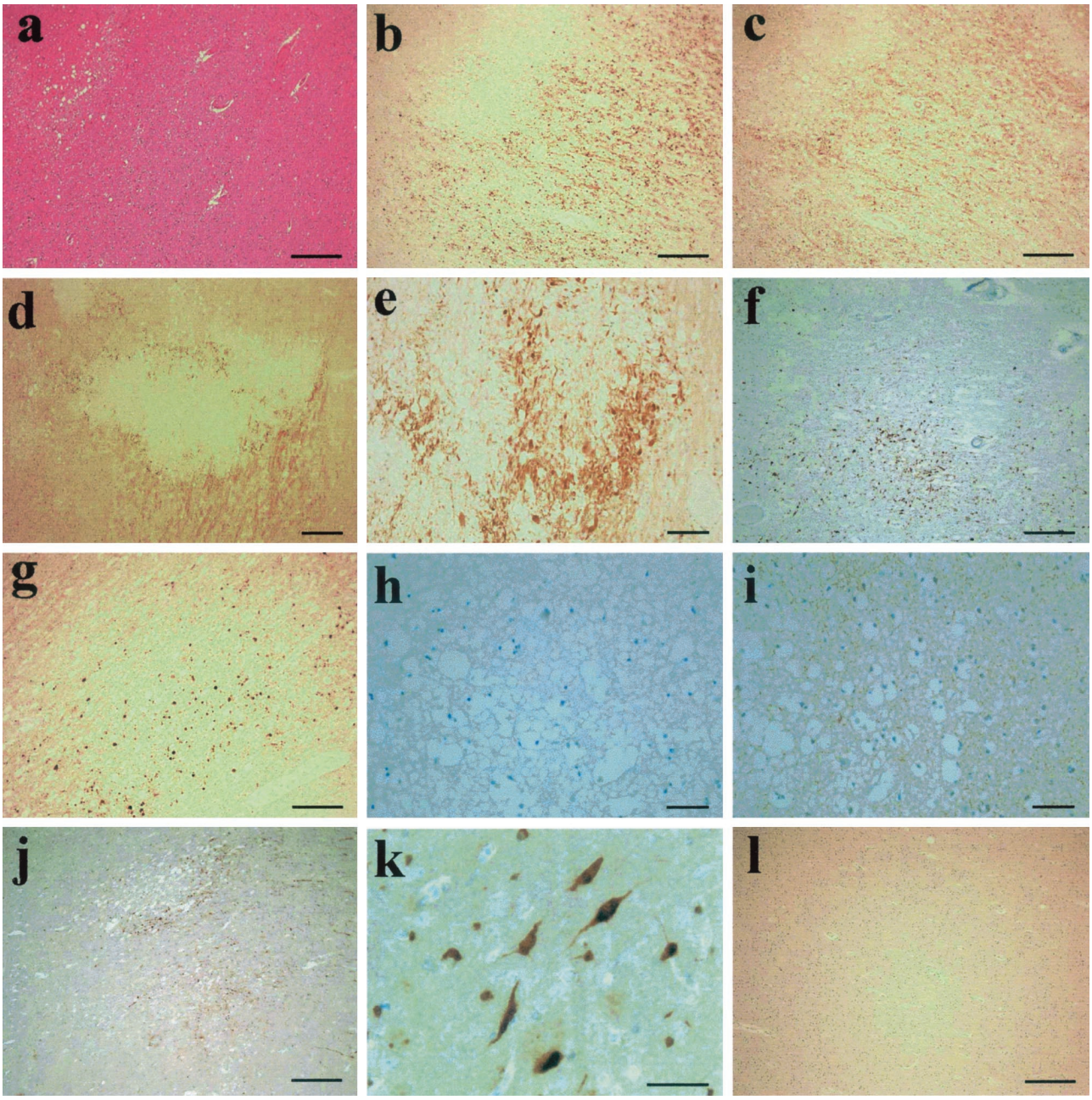

Figure 1. Immunohistochemistry on the adult CI cases. **a:** H&E staining of an ischemic lesion, case A3. The same lesion was probed for PrP using 3F4 (**b**) and βAPP using MAB348 (**c**). **d:** Another lesion probed with 3F4 demonstrating both axonal- and punctate-type staining patterns (case A1). **e:** A higher power view of the axonal PrP staining seen in several cases (case A7). **f** and **g:** Case A4 (**f**) and case A12 (**g**) show typical patterns of intense punctate PrP deposition in penumbra of ischemic damage. **h** and **i:** Case A6 demonstrates the widespread punctate PrP staining that was seen in all cases adjacent to ischemic lesions, with **h** being the no primary antibody control of the same region for contrast. **j:** The similar staining pattern of PrP deposition seen in the vicinity of a gray matter lesion (case A1). **k:** A small cluster of neurons strongly positive for PrP protein in the gray matter of an affected case (case A1). **l:** A normal piece of tissue stained for PrP using 3F4 for comparison. Scale bars: 500 μm (**d**); 250 μm (**a–c**, **f**, **g**, **j**, **l**); 100 μm (**e**); 50 μm (**h**, **i**, **k**).

The infarct contained no recognizable neurons but many vacuolated cell profiles with a small, dark, pyknotic nucleus; an appearance typical of cells that have undergone ischemic cell death.[31] The only surviving neurons were found at the edges of the lesion. Extensive neuronal loss was seen in the striatum of the PrP-null mice, but not in the wild-type mice or the PrP$^{+/0}$ heterozygous cross.

Tetrazolium blue chloride staining of brain slices from 129/Ola mice (PrP$^{+/+}$) and the PrP-null (129/Ola PrP$^{0/0}$) mice revealed that in PrP-null mice the cortical damage consistently extended further dorsally and ventrally than in wild-type mice (129/Ola PrP$^{+/+}$). The lesion extended into the striatum in the PrP$^{0/0}$ null mice but not in the wild-type mice (Figure 3). The lesion in 129/Ola PrP$^{+/0}$ heterozygous mice was intermediate between those of the null and wild-type mice. Further studies revealed that the vascular structures in PrP$^{+/+}$, PrP$^{+/0}$, and PrP$^{0/0}$ mice was similar suggesting that the infarct volume depends on PrP expression rather than being mediated by a developmental difference in cerebral vasculature between the three lines (Figure 4).

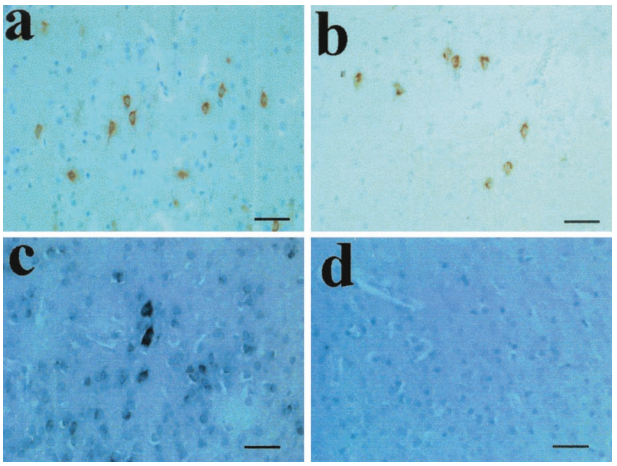

Figure 2. Immunohistochemistry and *in situ* hybridization on cases of HII. **a** and **b:** PrP staining of hypoxic neurons using 3F4 on cases P1 and P3, respectively. **c:** The *in situ* hybridization signal seen for PrP mRNA in case P3 coinciding with cells positive for PrP protein. **d:** The *in situ* hybridization sense control probe. Scale bars, 50 μm.

Statistical analysis showed a highly significant increase of 50%, in the size of the infarct between the $PrP^{0/0}$ and the $PrP^{+/+}$ mice [$PrP^{+/+}$ = 31.3 (±4.3) mm^3; $PrP^{0/0}$ = 47.5 (±7.5) mm^3; analysis of variance: F = 35.39, df = 2.39, $P < 0.0001$]. There was no significant difference between the $PrP^{+/+}$ and the $PrP^{0/0}$ mice in terms of the amount of swelling of the injured hemisphere (data not shown). Reintroduction of the PrP gene into the PrP-null background by breeding with the wild-type mice of the same mouse strain (129/Ola) reduced the lesion size to 40.7 (±3.3) mm^3, ie, by ~50% of the difference between the lesion size between null and wild-type mice (Table 4). LSD (least significant difference, post hoc multiple comparison) showed significant differences between each of the three groups of mice.

PrP Immunocytochemistry and in Situ *Hybridization*

In nonoperated mice, and in the contralateral hemisphere of mice with the MCA occlusion, PrP^c was detected as a faint punctate staining of occasional neuronal perikarya, as reported previously.[32] In contrast, within the penumbra of the infarct, where the neurons are sublethally damaged, many neurons showed PrP immunoreactivity with both PrP antibodies used. In addition, PrP immunoreactivity was associated with neuronal cell bodies and as diffuse, punctate staining of the neuropil in the ischemic hemisphere (Figure 5a). Similar increases in PrP immunoreactivity have also been observed in response to MCA occlusion in C57BL mice (Williams A, Davies I, Fotheringham A; data not presented) and in normal rats (Horsburgh K, Wellcome Surgical Institute, Glasgow; and Williams A, data not shown). No PrP immunoreactivity was present in the core of the infarct and no increases in PrP staining were seen in the contralateral

Table 4. Mouse Genotype and Infarct Volume

Strain of mouse	Mean infarct volume (mm^3)	SD	*n*
129/Ola $PrP^{+/+}$	31.3	4.3	19
129/Ola $PrP^{0/0}$	47.5	7.5	17
129/Ola $PrP^{+/0}$	40.7	3.3	6

129/Ola $PrP^{+/+}$ *versus* 129/Ola $PrP^{0/0}$, 129/Ola $PrP^{+/0}$ *versus* 129/Ola $PrP^{0/0}$, 129/Ola $PrP^{+/+}$ *versus* 129/Ola $PrP^{+/0}$.
t = −6.11, df = 24.3 (corrected for unequal variance), $P < 0.0001$.

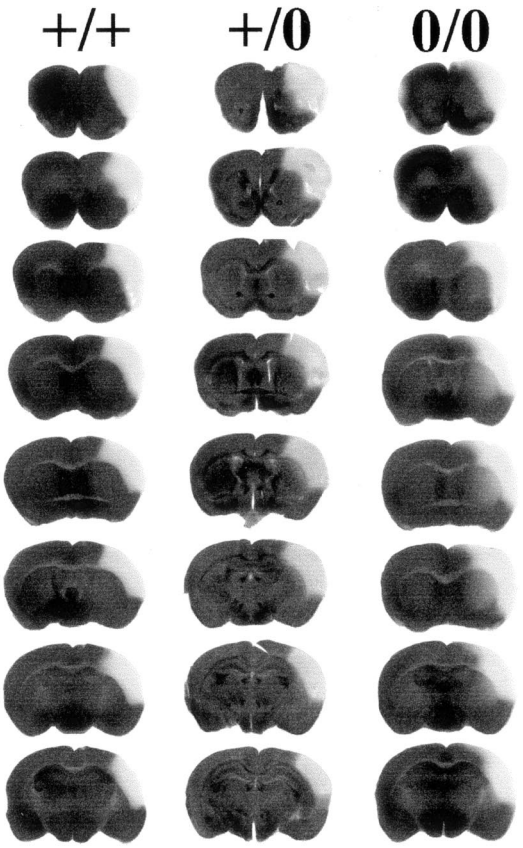

Figure 3. Serial slices through the infarcted brain after staining with tetrazolium blue chloride. Serial slices from co-ordinates F +1.8 to F −1.6. The damaged regions can be seen as pale areas on the left-hand hemisphere. It can be seen that the damage in the $PrP^{0/0}$ mice is more widespread than the other two lines. Note that the full range of the damaged area has not been shown. The data shown in Table 4 includes all slices with damage. **Left**, $PrP^{+/+}$; **middle**, $PrP^{+/0}$; and **right**, $PrP^{0/0}$.

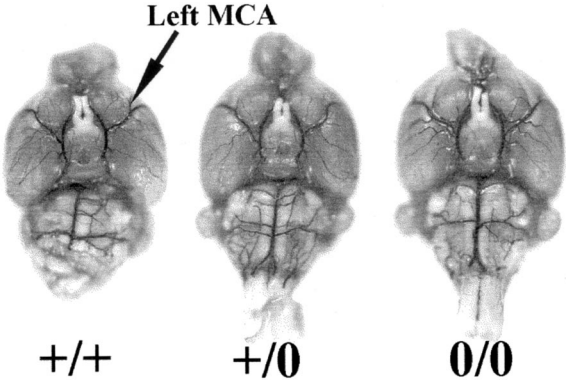

Figure 4. Vascular structure determination using latex filling. The circle of Willis and the left and right MCA in three strains of the 129Ola mouse after the vascular system was filled with latex colored with Indian ink. Four mice were analyzed of each genotype. The vascular structure relating to the MCA is closely similar in the three strains analyzed. **Left**, $PrP^{+/+}$; **center**, $PrP^{+/0}$; and **right**, $PrP^{0/0}$.

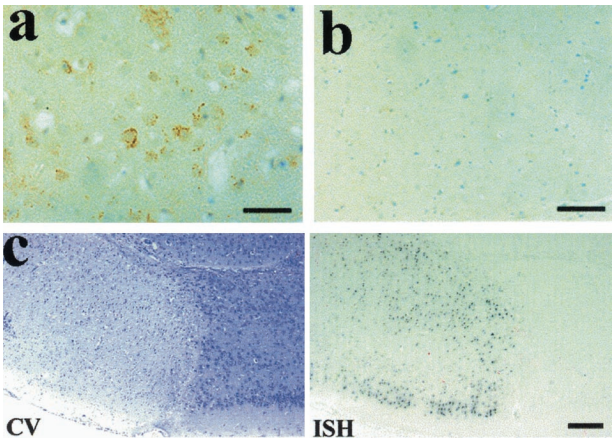

Figure 5. Analysis of MCA occlusion in the mouse. **a:** The PrP signal from the ischemic region of the mouse brain showing large amounts of protein deposition. **b:** The contralateral control region treated with the same antibodies. **c:** A cresyl violet stain (CV) showing the ischemic lesion as a pale area (**left**) and the *in situ* hybridization signal for PrP mRNA from the cells in the penumbra of the lesion (**right**). Scale bars: 100 μm (**a**, **b**); 200 μm (**c**).

side of the brain in ischemic (Figure 5b) or nonoperated mice. The use of normal rabbit sera and antibodies raised against irrelevant antigens failed to show any staining indicating the specificity of the anti-PrP antibodies.

In situ hybridization showed a similar increase in PrP mRNA expression to that observed for the increased PrP immunoreactivity. Thus at longer exposure (length of the chromogen staining step) times, *in situ* hybridization positivity was seen in all neuronal populations within the brain. However, when exposure times were reduced so that the alkaline phosphatase signal from normal (eg, contralateral hemisphere) neurons was not visible, strong reactivity was still evident in the penumbral neurons of the ischemic lesion in 129/Ola PrP$^{+/+}$ mice (Figure 5c). No mRNA signal was detected in the 129/Ola PrP$^{0/0}$ mice at the longer or shorter exposure times.

Discussion

Although the biological function of the prion protein remains unknown, several lines of research have suggested a protective role for PrP^C in the cellular response to oxidative damage. Neuronally expressed PrP^C is axonally transported and thus may have an involvement in the response of white matter to hypoxic events. Here we report the presence of PrP^C immunoreactivity within axons in the penumbra of foci of white matter damage and within neuronal soma in gray matter damage in human CI and hypoxia. The histopathology associated with the immunostaining observed in our study was characteristic of hypoxic damage and not prion disease, suggesting that our findings are not because of the presence of the disease related isoform, PrP^{Sc}. Furthermore, preliminary Western blot studies demonstrate that the molecular characteristics of the PrP expressed within hypoxic brain tissue are not those of PrP^{Sc} (P.M. Brennan, A. McNeill, and N.F. McLennan, unpublished observations). These results, taken with the study of Esiri and colleagues,[33] which concluded that cellular PrP might be up-regulated in the human brain under injurious conditions, lead us to propose that the observed pattern of PrP immunostaining in hypoxic human brain reflects the presence of PrP^C.

In the CI cases PrP^C accumulation was observed in all positive cases as a punctate background of immunopositivity and in addition in half the cases much of the PrP is seen within damaged axons in the brain, frequently coinciding with βAPP immunopositivity. The βAPP protein is known to be up-regulated during CI and to accumulate within damaged axons as a result of disrupted anterograde axonal transport.[34,35] Thus, PrP^C expression within hypoxic lesions might simply represent a passive result of deranged neuronal protein trafficking rather than an induced response to injury. However, because neuronal somata also displayed PrP^C immunostaining, it is possible that PrP^C synthesis is increased after hypoxia, even if in some cases cytoskeletal damage is contributing physically toward the axonal accumulation. Thus, it is likely that the axonal co-localization of βAPP and PrP^C are independent consequences of the ischemic injury rather than demonstrative of a functional relationship. It is interesting to note that in some (but not all) cases of Alzheimer's disease PrP^C and the amyloid β fragment co-localize in amyloid plaques,[36] although the significance of this observation is unclear at present.

In our study 10 of the 12 cases of adult CI showed immunopositivity for PrP. The two negative cases were not similar in that the disease durations were very different (<24 hours *versus* 28 days). There are many potential variables in the human samples used here such as time variables, sample age, degree of fixation, and sample handling, which could contribute to the variations seen in all of the cases, however it seems most likely that the location of the ischemic lesion plays a major role in determining the resulting cellular responses and therefore it could be argued that these cases are not directly comparable. Nevertheless our finding that PrP accumulation is seen in almost all of these diverse cases is most striking.

In situ hybridization analysis of a perinatal HII case demonstrated an increased PrP mRNA signal in those regions containing PrP^C immunostaining neurons. We propose that the most likely mechanism to account for the observed neuronal immunoreactivity of PrP^C accumulation is a transcriptional up-regulation of prion protein gene expression. This suggestion is backed up by research from Shyu and colleagues,[37] although a decrease in mRNA turnover in these cells cannot be excluded. The transcriptional stimuli regulating PrP^C expression are unknown, although inflammatory cytokines and reactive oxygen species, both of which induce PrP^C *in vitro*[18,38] are produced within the penumbra of ischemic lesions. Further analysis of this phenomenon and the utilization of cell culture and animal models will allow us to address these questions more directly.

The studies of experimental ischemia in mice (permanent middle artery occlusion) confirmed the results obtained on human tissue. In mice, increased PrP mRNA and PrP immunoreactivity were seen associated with neuronal soma in the penumbra of the ischemic lesion. The difference in cellular location between the mouse model and human material could reflect the fact that the

lesion in the mice was more acute and affected a greater relative proportion of the brain so that the increased PrP^C was detected in neuronal cell bodies only, and not in axons after subsequent transport down neuronal processes.

The functional importance of PrP^C, with a protective role after neuronal injury, was further emphasized in studies using PrP-null mice. All of the mice used in this study had an inbred 129/Ola background[39] allowing us to make direct and accurate comparisons of the lesion size in wild-type 129/Ola ($PrP^{+/+}$) and PrP-null (129/Ola $PrP^{0/0}$) mice without confounding factors because of diverse genetic backgrounds. The lesion size in the 129/Ola $PrP^{+/+}$ and in the 129/Ola $PrP^{0/0}$ mice was highly reproducible, with only a small range in lesion size within the genotypes (but differing volumes between genotypes). These differences could not be attributed to variations in vascular structures because it was shown that these structures are similar in $PrP^{+/+}$, $PrP^{+/0}$, and $PrP^{0/0}$ mice. The lesion was significantly larger in $PrP^{0/0}$ mice compared to mice of the same strain but possessing either one or two copies of the PrP gene. This increase in lesion size in the PrP-null mice would support the hypothesis that some neuronal populations sublethally damaged in mice containing a functional PrP gene, but able to survive, were not able to do so when devoid of PrP. Reintroduction of a single PrP allele, as in the hemizygous mice, was only partially protective suggesting a quantitative effect in which the level of PrP^C is limiting, further reinforcing a potential neuroprotective role for the protein.

Injured neurons increase synthesis of protective proteins and decrease production of nonessential molecules,[40] and so our data supports the hypothesis that PrP^C may have a neuroprotective role. Although other reports suggest a role for PrP in the oxidative stress response, it is not possible from these results to dissect out a distinct biochemical function for PrP^C in the hypoxically injured brain. Understanding the physiological role of PrP^C may help to elucidate the pathological processes associated with the prion diseases, and consequently suggest treatment strategies. PrP^{Sc}, the disease-associated isoform of prion protein, may have an aberrant neuroprotective function resulting from alteration in its secondary structure compared to PrP^C. Indeed, prion infected cells have been shown to exhibit increased susceptibility to oxidative damage.[24,41,42] Oxidative stress has also been implicated in the pathogenesis of a number of human neurodegenerative conditions, such as Parkinson's disease, Huntington's disease, Alzheimer's disease, and amyotrophic lateral sclerosis[43,44] and so PrP^C may also play a part in these conditions. Further analysis of PrP^C expression and function in normal and diseased brain tissues, in cell culture and in animal models of hypoxia and other neurological conditions may provide further understanding of the role of PrP in this and other neurological conditions.

Acknowledgments

We thank Linda McCardle and the staff of the National Creutzfeldt-Jakob Disease Surveillance Unit, University of Edinburgh, and Ms. Selma Rebus, Department of Veterinary Pathology, University of Glasgow, for the skilled assistance; D. Dewar and D. Graham, Department of Neuropathology, Southern General Hospital, University of Glasgow, for their contribution to the early stages of this study; J. Manson, Institute for Animal Health, Edinburgh, for supplying the PrP-null mice and 129/Ola wild-type mice; and R. Kascsak, New York State Institute for Basic Research in Developmental Disabilities, Staten Island, NY, for the gift of R9 and R27 antibodies.

References

1. Prusiner SB: Prions. Proc Natl Acad Sci USA 1998, 95:13363–13383
2. Brown DR, Qin K, Herms JW, Madlung A, Manson J, Strome R, Fraser PE, Kruck T, von Bohlen A, Schulz-Schaeffer W, Giese A, Westaway D, Kretzschmar H: The cellular prion protein binds copper in vivo. Nature 1997, 390:684–687
3. McLennan NF, Rennison KA, Bell JE, Ironside JW: In situ hybridization analysis of PrP RNA in human CNS tissues. Neuropath Appl Neurobiol 2001, 27:373–383
4. Sales N, Rodolfo K, Hassig R, Faucheux B, Di Giamberardino L, Moya KL: Cellular prion protein localization in rodent and primate brain. Eur J Neurosci 1998, 10:2464–2471
5. Bendheim PE, Brown HR, Rudelli RD, Scala LJ, Goller NL, Wen GY, Kascsak RJ, Cashman NR, Bolton DC: Nearly ubiquitous tissue distribution of the Scrapie agent precursor protein. Neurology 1992, 42:149–156
6. Brown KL, Ritchie DL, McBride PA, Bruce ME: Detection of PrP in extraneural tissues. Microsc Res Tech 2000, 50:40–45
7. Pammer J, Weninger W, Tschachler E: Human keratinocytes express cellular prion-related protein in vitro and during inflammatory skin diseases. Am J Pathol 1998, 153:1353–1358
8. Shmakov AN, McLennan NF, McBride P, Farquhar CF, Bode J, Rennison KA, Ghosh S: Cellular prion protein is expressed in the human enteric nervous system. Nat Med 2000, 6:840–841
9. Bueler H, Fischer M, Lang Y, Bluethmann H, Lipp HP, DeArmond SJ, Prusiner SB, Aguet M, Weissmann C: Normal development and behaviour of mice lacking the neuronal cell-surface PrP protein. Nature 1992, 356:577–582
10. Cashman NR, Loertscher R, Nalbantoglu J, Shaw I, Kascsak RJ, Bolton DC, Bendheim PE: Cellular isoform of the scrapie agent protein participates in lymphocyte activation. Cell 1990, 61:185–192
11. Reilly CE: Nonpathogenic prion protein acts as a cell-surface signal transducer. J Neurol 2000, 247:819–820
12. Manson J, West JD, Thomson V, McBride P, Kaufman MH, Hope J: The prion protein gene: a role in mouse embryogenesis? Development 1992, 115:117–122
13. Herms J, Tings T, Gall S, Madlung A, Giese A, Siebert H, Schurmann P, Windl O, Brose N, Kretzschmar H: Evidence of presynaptic location and function of the prion protein. J Neurosci 1999, 19:8866–8875
14. Cagampang FR, Whatley SA, Mitchell AL, Powell JF, Campbell IC, Coen CW: Circadian regulation of prion protein messenger RNA in the rat forebrain: a widespread and synchronous rhythm. Neuroscience 1999, 91:1201–1204
15. Tobler I, Gaus SE, Deboer T, Achermann P, Fischer M, Rulicke T, Moser M, Oesch B, McBride PA, Manson JC: Altered circadian rhythms and sleep in mice devoid of prion protein. Nature 1996, 380:639–642
16. Collinge J, Whittington MA, Sidle KC, Smith CJ, Palmer MS, Clarke AR, Jefferys JG: Prion protein is necessary for normal synaptic function. Nature 1994, 370:295–297
17. Brown DR, Schmidt B, Kretzschmar HA: Effects of oxidative stress on prion protein expression in PC12 cells. Int J Dev Neurosci 1997, 15:961–972
18. Sauer H, Dagdanova A, Hescheler J, Wartenberg M: Redox-regulation of intrinsic prion expression in multicellular prostate tumor spheroids. Free Radic Biol Med 1999, 27:1276–1283
19. Shyu WC, Kao MC, Chou WY, Hsu YD, Soong BW: Heat shock

modulates prion protein expression in human NT-2 cells. Neuroreport 2000, 11:771–774
20. Brown DR, Schmidt B, Kretzschmar HA: Effects of copper on survival of prion protein knockout neurons and glia. J Neurochem 1998, 70:1686–1693
21. White AR, Collins SJ, Maher F, Jobling MF, Stewart LR, Thyer JM, Beyreuther K, Masters CL, Cappai R: Prion protein-deficient neurons reveal lower glutathione reductase activity and increased susceptibility to hydrogen peroxide toxicity. Am J Pathol 1999, 155:1723–1730
22. Brown DR, Nicholas RSJ, Canevari L: Lack of prion protein expression results in a neuronal phenotype sensitive to stress. J Neurosci Res 2002, 67:211–224
23. Klamt F, Dal-Pizzol F, Conte da Frota MLJR, Walz R, Andrades ME, da Silva EG, Brentani RR, Izquierdo I, Fonseca Moreira JC: Imbalance of antioxidant defense in mice lacking cellular prion protein. Free Radic Biol Med 2001, 30:1137–1144
24. Wong BS, Liu T, Li R, Pan T, Petersen RB, Smith MA, Gambetti P, Perry G, Manson JC, Brown DR, Sy MS: Increased levels of oxidative stress markers detected in the brains of mice devoid of prion protein. J Neurochem 2001, 76:565–572
25. Giese A, Kretzschmar HA: Prion-induced neuronal damage—the mechanisms of neuronal destruction in the subacute spongiform encephalopathies. Curr Top Microbiol Immunol 2001, 253:203–217
26. Guentchev M, Voigtländer T, Haberler C, Groschup M, Budka H: Evidence for oxidative stress in experimental prion disease. Neurobiol Disease 2000, 7:270–273
27. Wong BS, Pan T, Liu T, Li R, Petersen RB, Jones IM, Gambetti P, Brown DR, Sy MS: Prion disease: a loss of antioxidant function? Biochem Biophys Res Commun 2000, 275:249–252
28. Love S: Oxidative stress in brain ischemia. Brain Pathol 1999, 9:119–131
29. Touzani O, Roussel S, MacKenzie ET: The ischaemic penumbra. Curr Opin Neurol 2001, 14:83–88
30. Fotheringham AP, Davies CA, Davies I: Oedema and glial cell involvement in the aged mouse brain after permanent focal ischaemia. Neuropathol Appl Neurobiol 2000, 26:412–423
31. Majno G, Joris I: Apoptosis, oncosis and necrosis: an overview of cell death. Am J Pathol 1995, 146:3–15
32. Bruce ME, McBride PA, Farquhar CF: Precise targeting of the pathology of the sialoglycoprotein, PrP, and vacuolar degeneration in mouse scrapie. Neurosci Lett 1989, 102:1–6
33. Esiri MM, Carter J, Ironside JW: Prion protein immunoreactivity in brain samples from an unselected autopsy population: findings in 200 consecutive cases. Neuropathol Appl Neurobiol 2000, 26:273–284
34. Baiden-Amissah K, Joashi U, Blumberg R, Mehmet H, Edwards AD, Cox PM: Expression of amyloid precursor protein (beta-APP) in the neonatal brain following hypoxic ischaemic injury. Neuropathol Appl Neurobiol 1998, 24:346–352
35. Stephenson DT, Rash K, Clemens JA: Amyloid precursor protein accumulates in regions of neurodegeneration following focal cerebral ischemia in the rat. Brain Res 1992, 593:128–135
36. Voigtländer T, Kloppel S, Birner P, Jarius C, Flicker H, Verghese-Nikolakaki S, Sklaviadis T, Guentchev M, Budka H: Marked increase of neuronal prion protein immunoreactivity in Alzheimer's disease and human prion diseases. Acta Neuropathol 2001, 101:417–423
37. Shyu WC, Harn HJ, Saeki K, Kubosaki A, Matsumoto Y, Onodera T, Chen CJ, Hsu YD, Chiang YH: Molecular modulation of expression of prion protein by heat shock. Mol Neurobiol 2002, 26:1–12
38. Satoh J, Kurohara K, Yukitake M, Kuroda Y: Constitutive and cytokine-inducible expression of prion protein gene in human neural cell lines. J Neuropath Exp Neurol 1998, 57:131–139
39. Manson JC, Clarke AR, Hooper ML, Aitchison L, McConnell I, Hope J: 129/Ola mice carrying a null mutation in PrP that abolishes mRNA production are developmentally normal. Mol Neurobiol 1994, 8: 121–127
40. Papadopoulos MC: An introduction to the changes in gene expression that occur after cerebral ischaemia. Br J Neurosurg 2000, 14: 305–312
41. Milhavet O, McMahon HE, Rachidi W, Nishida N, Katamine S, Mange A, Arlotto M, Casanova D, Riondel J, Favier A, Lehmann S: Prion infection impairs the cellular response to oxidative stress. Proc Natl Acad Sci USA 2000, 97:13937–13942
42. Thackray AM, Knight R, Haswell SJ, Bujdoso R, Brown DR: Metal imbalance and compromised antioxidant function are early changes in prion disease. Biochem J 2002, 362:253–258
43. Beal MF: Aging, energy and oxidative stress in neurodegenerative diseases. Ann Neurol 1995, 38:357–366
44. Smith MA, Rottkamp CA, Nunomura A, Raina AK, Perry G: Oxidative stress in Alzheimer's disease. Biochim Biophys Acta 2000, 1502: 239–244